Soft photon production in central 200 GeV/nucleon ^{32}S + Au collisions

M. M. Aggarwal,[1] A. L. S. Angelis,[2] V. Antonenko,[3] T. C. Awes,[4] S. K. Badyal,[5] C. Barlag,[6] K. B. Bhalla,[7] V. S. Bhatia,[1] C. Blume,[6] D. Bock,[6] E.-M. Bohne,[6] D. Bucher,[6] A. Buijs,[8] S. Chattopadhyay,[9] A. Claussen,[6] G. Clewing,[6] A. C. Das,[9] Devanand,[5] P. Dönni,[2] E. Durieux,[2] M. R. Dutta Majumdar,[9] P. Foka,[2] S. Fokin,[3] M. S. Ganti,[9] S. Garpman,[10] F. Geurts,[8] T. K. Ghosh,[9] R. Glasow,[6] S. K. Gupta,[7] H.-Å. Gustafsson,[10] H. H. Gutbrod,[11,*] M. Hartig,[6] He Xiaochun,[12] G. Hölker,[6] M. Ippolitov,[3] M. Izycki,[2] S. Kachroo,[5] H. Kalechofsky,[2] R. Kamermans,[8] K.-H. Kampert,[6,†] K. Karadjev,[3] B. W. Kolb,[11] V. Kumar,[7] I. Langbein,[11] J. Langheinrich,[6] A. Lebedev,[3] H. Löhner,[13] S. Lokanathan,[7] V. Manko,[3] M. Martin,[2] I. S. Mittra,[1] S. Mookerjee,[7] H. Naef,[2] S. K. Nayak,[9,‡] S. Nikolaev,[3] J. Nystrand,[10] F. E. Obenshain,[4] A. Oskarsson,[10] I. Otterlund,[10] T. Peitzmann,[6] F. Plasil,[4] M. Purschke,[11,§] S. Raniwala,[7] N. K. Rao,[5] L. Rosselet,[2] B. Roters,[11] J. M. Rubio,[2] S. Saini,[4] S. S. Sambyal,[5] R. Santo,[6] H. R. Schmidt,[11] T. Siemiarczuk,[14] R. Siemssen,[13] B. C. Sinha,[9] S. Slegt,[13] K. Söderström,[10] N. Solomey,[2] S. P. Sorensen,[11] G. Stefanek,[14] P. Steinhaeuser,[11] E. Stenlund,[10] A. Ster,[2] D. Stüken,[6] M. D. Trivedi,[9] C. Twenhoefel,[8] N. van Eijndhoven,[8] E. van Heeringen,[8] A. Vinogradov,[3] Y. P. Viyogi,[9] S. Weber,[6,‖] and G. R. Young[4]
(WA93 Collaboration)

[1]*University of Panjab, Chandigarh 160014, UT, India*
[2]*University of Geneva, CH-1211 Geneva 4, Switzerland*
[3]*Kurchatov Institute, RU-123182 Moscow, Russia*
[4]*Oak Ridge National Laboratory, Oak Ridge, Tennessee 37831-6372*
[5]*University of Jammu, Jammu 180001, India*
[6]*University of Münster, D-48149 Münster, Germany*
[7]*University of Rajasthan, Jaipur 302004, Rajasthan, India*
[8]*University of Utrecht, NL-3508 TA Utrecht, The Netherlands*
[9]*Variable Energy Cyclotron Centre, Calcutta 700 064, India*
[10]*University of Lund, S-223 62, Sweden*
[11]*Gesellschaft für Schwerionenforschung (GSI), D-64220 Darmstadt, Germany*
[12]*University of Tennessee, Knoxville, Tennessee 37996*
[13]*KVI, University of Groningen, NL-9747 AA Groningen, The Netherlands*
[14]*Institute of Nuclear Studies, PL-00681 Warsaw, Poland*
(Received 12 September 1996)

Inclusive photons of low transverse momenta have been measured in 200 GeV/nucleon $^{32}S+Au$ collisions at the CERN SPS. Data were taken in the WA93 experiment using a small acceptance BGO detector with longitudinal segmentation. The results are compared to WA80 measurements for the same system and results from hadron decay calculations. An excess of soft photons over the expectations from neutral meson decays is observed. [S0556-2813(97)05007-3]

PACS number(s): 25.75.−q, 29.40.Mc

The production of photons in ultrarelativistic heavy ion collisions is of special interest because electromagnetic radiation from the hot system created in such reactions can leave the reaction volume undisturbed by hadronic interactions. Such *direct* photons may yield information from the early dense phase of the reaction. In order to disentangle a possible surplus of direct photons on top of the overwhelming photon background from hadronic decay photons, a careful study of the inclusive photon spectrum is mandatory. This analysis will provide insight into the various sources of hadronic decay background.

Limits on direct photons in 200 GeV/nucleon ^{32}S + Au collisions have recently been published by the WA80 Collaboration [1]. In the WA80 experiment photons were measured with a lead glass calorimeter, which has natural limitations for the measurement of low energy photons because the detection process relies on the Cherenkov effect. Therefore a small detector using BGO scintillating crystals was developed for the WA93 experiment. It consisted of an 8×8 matrix of 64 crystals each with a cross section of 25×25 mm^2 (approximately 1 Molière radius) and a length of 250 mm (22 radiation lengths). Part of these crystals (35) were longitudinally segmented (70 mm + 180 mm), which yielded additional information about the longitudinal shower development and thus improved the hadron rejection particu-

*Now at Subatech, Ecole des Mines de Nantes, France.
†Now at University of Karlsruhe, D-76131 Karlsruhe, Germany.
‡Present address: Nuclear Science Center, New Delhi, India.
§Now at Brookhaven National Laboratory, Upton, NY 11973.
‖Now at Forschungszentrum Jülich, D-52425 Jülich, Germany.

 © 1997 The American Physical Society

larly at low incident energies. The light from the crystals was detected by two p-i-n photodiodes (four in the case of segmented crystals), which were read out via custom-designed preamplifiers, shaping amplifiers [2], and commercial analog-to-digital converters (ADC's). The detector was embedded in a sophisticated temperature stabilization system, ensuring a stability of better than 0.1 K. A xenon flasher and an electronic pulser were used to monitor the signal of each readout channel. Details about the detector can be found in [3]. It was used successfully in the WA93 experiment to measure inclusive photon spectra. In this paper we present the results obtained for the most central 812 mb ($\approx$22.6 %) of the 200*A* GeV ^{32}S + Au cross section. The centrality selection was performed via the transverse energy measured with the Mid-Rapidity Calorimeter [4].

The WA93 experiment was a successor of the WA80 experiment and is described in detail in [5]. The setup was enlarged by adding the Photon Multiplicity Detector [6] and a magnetic spectrometer for negative particles which consisted of the magnet GOLIATH and four multistep avalanche chambers [7]. Furthermore, the BGO detector was added. It covered the pseudorapidity range between 2.35 and 2.45 and a range of approximately 7° in azimuth, and was positioned at a distance of 10 m from the target.

The energy signals from the BGO detector are processed by a clustering algorithm, which identifies hits and calculates their characteristics. It also allows to separate overlapping hits, when they are not closer then 1.8 module units [3].

In this study the identification of photons was performed with two different techniques: (1) the analysis of the lateral dispersion, which is significantly smaller for electromagnetic as compared to hadronic showers (*dispersion method*) [8], and (2) the analysis of the longitudinal depth of the energy distribution, which differs considerably for minimum ionizing particles and hadron showers on the one hand and electromagnetic showers with equivalent energy deposit on the other hand (*forward/total method*) [3].

As an example, the hadron rejection capabilities of the BGO detector are compared to those of the lead glass for particles depositing a total energy of 1 GeV in Table I. It can be seen that the lead glass has very little rejection power at this energy, while the BGO allows us to reject 80–99 % of the hadrons.

To study the detection efficiency, the GEANT [9] simulation package has been used to create artificial signals for the BGO modules corresponding to different particles hitting the detector. In total, $\sim$30 000 charged pions and $\sim$40 000 photons have been simulated with a uniform transverse momentum distribution. The momentum distributions have then been weighted according to the corresponding particle distributions obtained from VENUS 3.11 [10]. This event generator is known to reproduce fairly well the produced particle spectra.

The simulated particles are analyzed in a realistic particle density environment by being superposed onto real measured events. In this way effects of detector noise are also treated properly. The simulated showers are then analyzed with the same analysis routines as the real data.

However, adding a single simulated shower in a small acceptance detector already causes a significant change of the effective local particle multiplicity. To study particle density effects the signals have been superimposed onto measured central ^{32}S + Au reactions and onto empty events which only contain the detector noise. These two cases effectively correspond to average hit multiplicities (extrapolated to 2π) of $\approx$150 and $\approx$50, respectively, while the real central events correspond to a multiplicity of $\approx$100. A good estimate of the detection efficiency can therefore be obtained from an interpolation between the two cases studied using the simulated data. The difference in the number of detected photons for these two cases is below 20% for most of the momentum range and reaches 30% only for $p_T \leqslant 100$ MeV/c.

TABLE I. The hadron rejection capabilities for a photon loss of $\approx$10% for an energy deposition of 1 GeV.

Detector	Method	Photon loss (%)	Hadron rejection (%)
lead glass	dispersion	10.0$\pm$2.0	8.5$\pm$2.0
BGO	dispersion	10.1$\pm$0.7	81.5$\pm$1.3
BGO	F/T	10.1$\pm$0.7	89.9$\pm$1.2
BGO	combined	9.7$\pm$0.7	98.7$\pm$1.1

From the simulation we have in this way obtained the probabilities that (a) a photon is correctly identified or (b) a hadron is mistakenly identified as a photon. These probabilities are used to correct the measured distributions. The photon efficiency is above 80% for most of the p_T range. The hadron contamination is on the level of a few percent at medium and high p_T and reaches values of 50–70 % in the lowest p_T bin.

We assume that the following sources contribute to the systematic error of the photon measurement.

(1) Secondary particles may be produced somewhere in the experimental setup and contribute to the measured particle yield in the BGO detector. In the analysis no shower having its maximum in one of the border modules was used, which eliminates particles being scattered from material on the sides of the detector. Possible sources of background are therefore (i) target (250 mg/cm^2 Au) and target chamber window, (ii) the GOLIATH magnet, (iii) the multistep avalanche tracking chambers, (iv) streamer tube detectors for charged particles, and (v) $\approx$10 m of air. We have included all of the above material in a GEANT simulation using VENUS 4.12 reactions as input.

With the material included the number of particles detected in the lowest p_T bin increases by $\approx$50% without any lower energy cutoff. Imposing the energy cutoff of 50 MeV used in the analysis reduces the background to $\approx$10%. The second lowest bin has a similar background fraction while the background fraction decreases to below 5% for higher p_T.

(2) The lower cutoff in energy together with the energy resolution of the detector causes an uncertainty in the yield of the lowest bin of $<5\%$.

(3) For the calculation of the hadron contamination we have used VENUS simulations. The uncertainty in the hadron spectra relates to an uncertainty in this contamination. We have used the recent measurements of NA44 [11] which indicate a low p_T enhancement to estimate this uncertainty. The maximum enhancement they observe is $\approx$11% — assuming this as the uncertainty of the hadron yield relative to

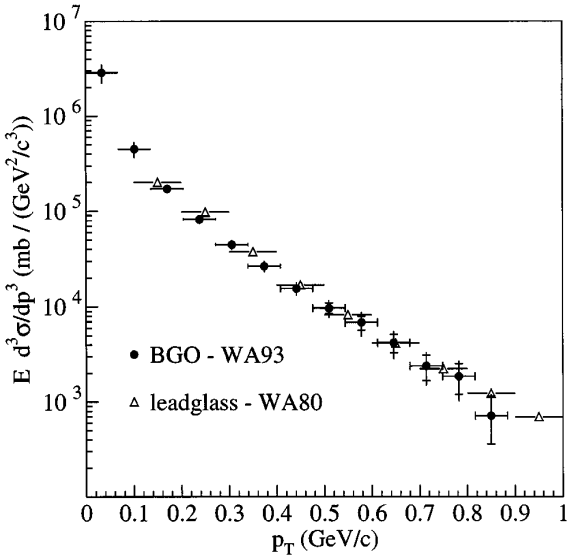

FIG. 1. Invariant cross section of inclusive photons for central reactions of 200*A* GeV S + Au as measured with the WA93 BGO detector (solid circles). The error bars contain both systematic and statistical errors added linearly. Also shown are data from the WA80 lead glass detector for a similar centrality selection (open triangles).

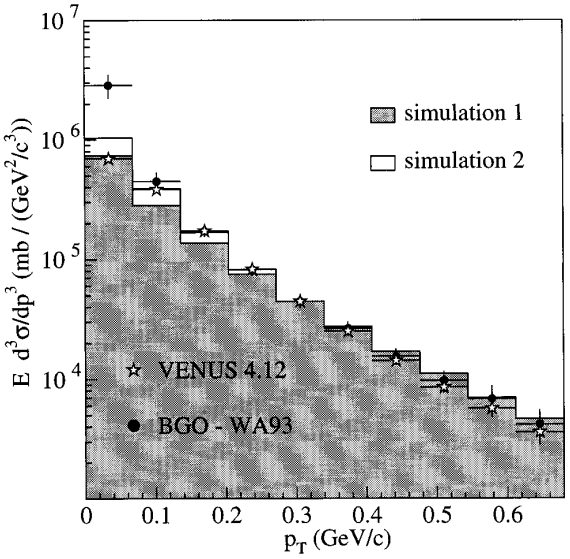

FIG. 2. Invariant cross section of inclusive photons for central reactions of 200*A* GeV S + Au as measured with the WA93 BGO detector (solid circles) as in Fig. 1. Included are results of VENUS simulations (stars). In addition, the histograms show results from a simulation of hadron decays normalized to the data for $p_T = 0.3$ MeV/c (see text).

photons we arrive at error contributions of 5.5–7.7 % for the lowest and 2.75–5.5 % for the second lowest bin depending on the particle identification method used.

(4) To estimate the systematic errors in the particle identification and efficiency correction, this study has been performed for different identification criteria, namely, by applying (a) only the dispersion method and (b) a combination of the dispersion method and the forward/total method.

The photon transverse momentum distributions, for the two methods after correction show a reasonable agreement with deviations of $< 18\%$, although the two uncorrected spectra are significantly different. For the lowest bin we have in addition analyzed hits with very small shower width, so that the dispersion method could not be applied. In this case only the forward/total method was used. We obtain a yield intermediate between the two other methods. Together we estimate the systematic error to be $\approx 10\%$ in the lowest bin and $\approx 6\%$ for the second lowest.

Adding all these contributions quadratically we end up with a total systematic error of 17% and 13% for the lowest and next lowest p_T bins, respectively. For higher p_T the error is below 8%. These estimates do not include the error on the total cross section ($\approx 20\%$), which would just change the overall normalization and would not affect the shape.

The final cross sections are extracted as the mean of the results obtained with the different identification methods weighted with their corresponding total error (statistic + systematic).

Figure 1 shows the cross section of inclusive photons for central reactions of 200*A* GeV S + Au as a function of the transverse momentum. Data from WA80 are included for comparison [1]. In the region of overlap both data sets are in good agreement. However, this measurement enlarges the low p_T extent of the photon measurement and provides an improved accuracy.

In Fig. 2 the data are displayed together with results from VENUS 4.12 normalized to the data at $p_T = 0.3$ GeV/c. They describe the data nicely at higher p_T, but are below the data at low p_T. One can also compare the low p_T cross section of inclusive photons with the expectation from hadron decays. For this purpose we have taken preliminary π^0 spectra measured by WA80 [12] for ^{32}S + Au and calculated the decay photons from π^0, η, η', and ω, where m_T scaling, following the method used in [1], was applied for the heavier mesons. Below $p_T = 0.8$ GeV/c the π^0 spectrum has been extrapolated with an exponential in m_T of inverse slope parameter $T = 210$ MeV. The decay photon spectrum has been normalized to the measured distribution for $p_T = 0.3$ GeV/c. The result is included in Fig. 2 as a gray histogram (simulation 1). While the shape of the inclusive photon spectrum is well

TABLE II. The photon excess relative to different reference distributions integrated over different regions of transverse momentum. The errors given include statistical and systematic errors added in quadrature.

Reference distribution	$R(p_T \leq 0.068$ GeV/$c)$	$R(p_T \leq 0.884$ GeV/$c)$	$R(0.068$ GeV/$c \leq p_T \leq 0.884$ GeV/$c)$
VENUS 4.12	3.12 ± 0.82	0.53 ± 0.16	0.07 ± 0.07
Simulation 1	2.89 ± 0.78	0.65 ± 0.17	0.18 ± 0.08
Simulation 2 ($T_2 = 100$ MeV)	1.75 ± 0.55	0.40 ± 0.14	0.05 ± 0.07

described by the decay photons for $p_T > 0.5$ GeV/c, the measured photon yield deviates from this prediction for lower transverse momenta — the measured yield is significantly larger.

However, also in the WA80 pion spectra there is an indication of an excess over the fitted function for the lowest p_T bin. We have therefore tried a modified function which includes a second exponential in m_T. This function fits the experimental π^0 spectra very well using a slope parameter of $T_2 = 100$ MeV [12]. The parameters of this second component are dominantly determined by the π^0 yield in the lowest bin at $p_T = 0.2 - 0.4$ GeV/c, which has an uncertainty of $\approx 30\%$. The additional component used here, while having an even slightly higher uncertainty because of the unknown π^0 yield below $p_T = 0.2$ GeV/c, comprises $\approx 20\%$ of the total integrated yield, and so in fact is a greater enhancement than the 11% enhancement quoted by NA44 [11]. The result of the simulation using this function is displayed as a white histogram (simulation 2) in Fig. 2. This simulation describes the data much better, but still the measured photons for $p_T \leq 68$ MeV/c exceed the simulation.

In Table II the relative photon excess defined as

$$R = \frac{\int_{p_T^{(\min)}}^{p_T^{(\max)}} dp_T dN_{\text{data}}/dp_T}{\int_{p_T^{(\min)}}^{p_T^{(\max)}} dp_T dN_{\text{ref}}/dp_T} - 1 \qquad (1)$$

is given for the first bin and for the full p_T range covered. One can see that even for the extreme case of the calculation including a low p_T enhancement there is a surplus of 1.75 in the first bin which is equivalent to 40% of the total yield.

While there is some uncertainty related to the determination of the low p_T shape of the pion spectrum, which is very much influenced by resonance production, it is unlikely that the large excess can be fully explained by a change in the pion spectrum. Additional mechanisms which may contribute at low p_T, e.g., the γ-decay modes of resonances (Δ, Σ) or contributions from bremsstrahlung, should be investigated. In fact, in a recent publication on measurements in hadron-nucleus collisions [13] the authors are able to describe their low p_T photon spectra with calculations of hadronic bremsstrahlung — such calculations are, however, beyond the scope of this paper.

The only other available measurement of photons in a comparable reaction (^{32}S + W,Pt) [14] reports no excess over hadronic sources for $p_T > 0.1$ GeV/c. For the most central collisions they investigate ($\langle E_T \rangle > 240$ GeV) one can extract a value of $R(p_T > 0.1 \text{ GeV}/c) = 0.063 \pm 0.155$ for the excess [Eq. (1)]. This is compatible with our measurement in the interval $0.068 \text{ GeV}/c \leq p_T \leq 0.884 \text{ GeV}/c$ given in Table II. This illustrates again that most of the photon excess is concentrated in the first p_T bin.

One can extract the average transverse momentum of the photons from the distribution of dN/dp_T, where a value of $\langle p_T \rangle = 159 \pm 15$ MeV/c is obtained.[1]

To summarize, inclusive photon spectra have been measured for $p_T < 1$ GeV/c in central ^{32}S + Au reactions with a small acceptance BGO detector. The complementary photon identification possibilities from both the dispersion method and the forward/total method allow to study the photon production down to low transverse momenta.

The experimental data show an enhancement compared to VENUS simulations and compared to decay calculations assuming an exponential shape of meson spectra at low m_T with an inverse slope of $T = 210$ MeV. Assuming a second component of $T = 100$ MeV would improve the description, but still would fail to describe the lowest p_T point.

We would like to thank the CERN-SPS accelerator crew for providing good sulfur beam conditions. This work was supported jointly by the German BMBF and DFG, the U.S. DOE, the Swedish NFR, the Dutch Stichting FOM, the Swiss National Fund, the Humboldt Foundation, the Stiftung für deutsch-polnische Zusammenarbeit, the Department of Atomic Energy, the Department of Science and Technology and the University Grants Commission of the Government of India, the Indo-FRG Exchange Program, the PPE division of CERN, the International Science Foundation under Contract NO. N8Y000, the INTAS under Contract No. INTAS-93-2773, and ORISE. ORNL is managed by Lockheed Martin Energy Research Corporation under Contract No. DE-AC05-96OR22464 with the U.S. Department of Energy.

[1]The error is dominated by the systematic errors from the efficiency and from binning effects.

[1] R. Albrecht *et al.*, Phys. Rev. Lett. **76**, 3506 (1996).
[2] A.L. Wintenberg *et al.*, IEEE Trans. Nucl. Sci. **NS-39**, 1286 (1992).
[3] K.-H. Kampert *et al.*, Nucl. Instrum. Methods Phys. Res. A **349**, 81 (1994).
[4] T.C. Awes *et al.*, Nucl. Instrum. Methods Phys. Res. A **279**, 479 (1989).
[5] WA93 Collaboration, Report No. CERN/SPSC/90-14, 1990; Report No. SPSC/P-252, 1990.
[6] M.M. Aggarwal *et al.*, Nucl. Instrum. Methods Phys. Res. A **372**, 143 (1996).
[7] M. Izicki *et al.*, Nucl. Instrum. Methods Phys. Res. A **310**, 98 (1991).
[8] F. Berger *et al.*, Nucl. Instrum. Methods Phys. Res. A **321**, 152 (1992).
[9] R. Brun *et al.*, GEANT3, CERN Data Handling Division, Report No. DD/EE/84-1, 1987.
[10] K. Werner, Phys. Rev. D **39**, 780 (1988).
[11] H. Bøggild *et al.*, Z. Phys. C **69**, 621 (1996).
[12] D. Stüken (unpublished).
[13] M.L. Tincknell *et al.*, Phys. Rev. C **54**, 1918 (1996).
[14] T. Åkesson *et al.*, Z. Phys. C **46**, 369 (1990).